Reaction Mechanisms

Unusual Nitrene Oxidation Product Formation by Metathesis Involving the Dioxygen O–O and Borylnitrene B–N Bonds

Virinder Bhagat, Julia Schumann, and Holger F. Bettinger*[a]

Abstract: The reaction of dioxygen with nitrenes can have significant energy barriers, although both reactants are triplet diradicals and the formation of nitroso-*O*-oxides is spin-allowed. By means of matrix-isolation infrared spectroscopy in solid argon, nitrogen, and neon, and through high-level computational quantum chemistry, it is shown herein that a 3-nitreno-1,3,2-benzodioxaborole CatBN (Cat = catecholato) reacts with dioxygen under cryogenic conditions thermally at temperatures as low as 7 K to produce two distinct products, an *anti*-nitroso-*O*-oxide and a nitritoborane CatBONO. The computed barriers for the formation of nitroso-*O*-oxide isomers are very low. Whereas *anti*-nitroso-*O*-oxide is kinetically trapped, its bisected isomer has a very low barrier for metathesis, yielding the CatBO + NO radicals in a strongly exothermic reaction; these radicals can combine under matrix-isolation conditions to give nitritoborane CatBONO. The trapped isomer, *anti*-nitroso-*O*-oxide, can form the nitritoborane CatBONO only after photoexcitation, possibly involving isomerization to the bisected isomer of *anti*-nitroso-*O*-oxide.

Introduction

Dioxygen is a very unusual molecule because it is an open-shell triplet diradical, but enjoys extraordinary persistence, which means it forms a substantial fraction of the earth's atmosphere. Almost all of its reactions, oxidations, are very exothermic due to the weak O–O σ bond, but often barriers are sufficiently high to preclude them.[1] This arises from the substantial 100 kcal mol^{-1} resonance energy of two three-electron, two-center π bonds.[1] Dioxygen, however, undergoes very fast reactions with other open-shell species, such as radicals and diradicals. Thus, the suppression of a reaction in the presence of oxygen is a qualitative test for the involvement of radicals. Likewise, the fast reaction of triplet carbenes with dioxygen, even at very low temperatures, as provided by matrix-isolation conditions, can serve as a qualitative test for the carbene spin state.[2]

It is well established that triplet aromatic nitrenes react much slower with oxygen than triplet aromatic carbenes.[3,4] According to the reports of Gritsan and Pritchina,[5] the rate of the reaction of *para*-substituted phenylnitrene and oxygen in solvents such as toluene and hexane is in the order of 10^{-6} L mol^{-1} s^{-1}. On the other hand, the reaction rate in the case of phenylcarbenes can reach the limit of diffusion control, even at low temperatures.[6] *p*-Aminophenylnitrene reacts to both the *syn*- and *anti*-*p*-aminophenylnitroso oxide (**2a** and **2b**, respectively) upon annealing of an argon matrix doped with 4% oxygen (Scheme 1a).[7] The isomers of *p*-aminophenylnitroso oxide were found to be photochemically interconvertible and, upon irradiation with $\lambda > 365$ nm, ultimately reacted to form *para*-nitroaniline.[7]

Remarkably, phenylnitrene undergoes no reaction, even in a solid O_2 matrix at 20 K, as shown by Sander et al.[8] Annealing in O_2-doped Xe matrix only consumed 40% of phenylnitrene, even after 12 h at 50 K, resulting mainly in the formation of *syn*-nitroso-*O*-oxide **2b** and finally nitrobenzene **4** after irradiating with visible light of wavelength 450 nm (Scheme 1a).[8] This indicates a high barrier for the reaction of molecular oxygen and phenylnitrene under matrix-isolation conditions. A computational study by Platz et al. explained the lower reactivity of phenylnitrene compared with that of phenylcarbene towards oxygen by thermodynamic arguments.[9]

However, not all nitrenes react reluctantly with molecular oxygen. For example, the parent nitrene, imidogen NH, is known to react in Xe matrix with O_2,[10] and a computational investigation agrees with the experimental results related to this reaction.[11] A particularly reactive nitrene is borylnitrene **6** CatBN (Cat = catecholato) formed in situ by irradiating matrix-isolated boryl azide **5**.[12] Nitrene **6** prefers a triplet electronic ground state, according to ESR spectroscopy and high-level computations.[12,13] Nitrene **6** and closely related borylnitrenes are very reactive towards sigma bonds (e.g., C(sp^3)–H, H–H) after *photoexcitation*, most likely due to the formation of the highly electrophilic singlet nitrene.[14–18] Borylnitrene **6**, however, also shows very high *thermal* reactivity towards O_2 in an

[a] V. Bhagat, Dr. J. Schumann, Prof. Dr. H. F. Bettinger
Institut für Organische Chemie, Universität Tübingen
Auf der Morgenstelle 18, 72076 Tübingen (Germany)
E-mail: holger.bettinger@uni-tuebingen.de

Supporting information and the ORCID identification number(s) for the author(s) of this article can be found under:
https://doi.org/10.1002/chem.202002445.

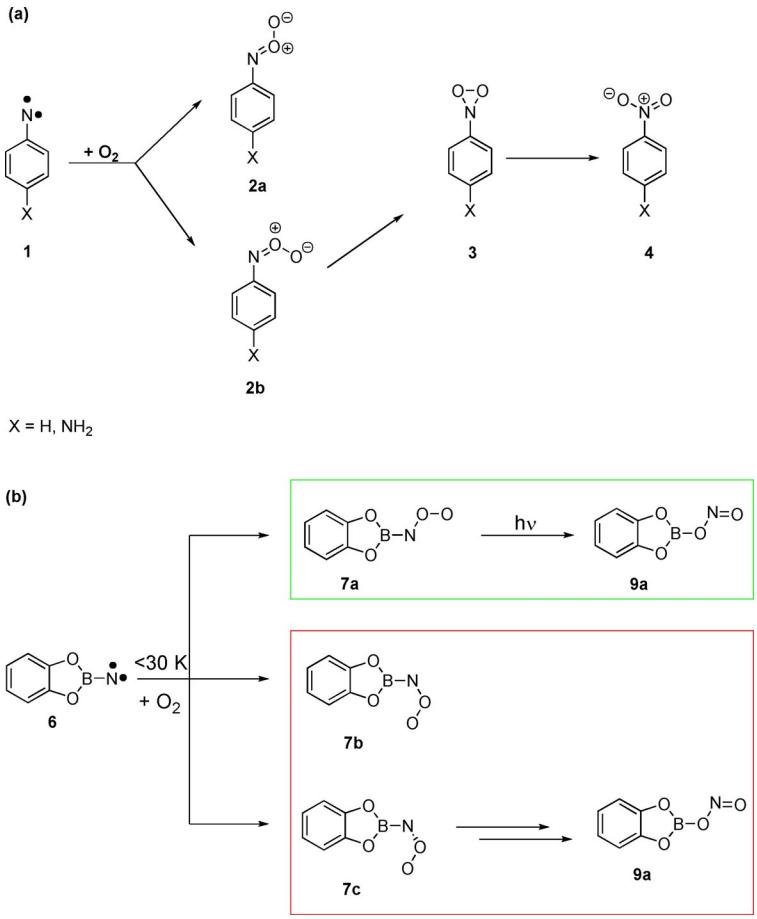

Scheme 1. a) Reaction of aromatic nitrenes **1** and the formation of nitroarenes **4** via intermediates **2a**, **2b**, and **3**. b) The reaction of borylnitrene **6** with oxygen and the formation of *anti*-nitritoborane **9a**. The portion enclosed in the green box corresponds to already explored aspects,[12] regarding the interaction of **6** with O_2, and that enclosed within the red box is unexplored and the subject of the present work.

argon matrix because annealing in the presence of O_2 quickly results in the formation of nitroso oxide **7a** (Scheme 1b).[12] The latter was shown to undergo, upon photoexcitation ($\lambda =$ 254 nm), a formal dyotropic rearrangement[19–21] to nitritoborane **9a**. Not only is the thermal reactivity of **6** towards O_2 higher than that of aryl nitrenes, but also the final oxidation product differs because not the nitro- ($CatBNO_2$) but the nitritoborane (CatBONO) is formed.[12] In addition, three isomers of nitroso oxide **7** could be identified computationally (UB3LYP/6-311+G**), but only conformation **7a** (*anti*) could be observed experimentally.[12] Neither the reason for the high reactivity of **6** towards oxygen upon annealing, nor the preference for the formation of **7a**, or even the mechanism of nitritoborane formation from nitroso oxide are currently known.

Herein, we show by combining matrix-isolation experiments and high-level computations that the thermal reaction of borylnitrene **6** with O_2 results in multiple products. Besides **7a**, which is kinetically locked under matrix-isolation conditions and only reacts upon subsequent photoexcitation, a low-barrier pathway via the bisected nitroso oxide isomer (**7c**) exists that allows the formation of a radical pair (**8**: CatBO+NO) by metathesis of the B–N and O–O bonds. The radical pair within the matrix cage eventually collapses to final product **9a**. Hence, it is possible for the system CatBN+O_2 to undergo simultaneous insertions into the B–N and O–O bonds to form CatBONO at temperatures as low as 30 K in argon and 7 K in Ne.

Experimental Section

Experiments

$CatBN_3$ was synthesized according to a published procedure.[22] Matrix-isolation experiments were performed by standard techniques on a Sumitomo SH-1 closed-cycle helium cryostat.[23] Matrices were produced by deposition of different materials, such as argon, nitrogen, and neon (Messer-Griesheim, 99.9999%), on top of a CsI (IR) window at 15, 10, and 4 K, respectively, with oxygen as a dopant (2–3%, 99.999% purity). IR spectra were recorded with a Bruker Vertex 70 FTIR spectrometer with a standard resolution of 0.5 cm^{-1} in the range of 400–4000 cm^{-1}. Irradiations were carried out by using a low-pressure mercury lamp ($\lambda = 254$ nm, PenRay).

Computations

Geometries of stationary points were optimized at the B3LYP level,[24,25] as implemented in Gaussian 16,[26] in conjunction with the 6-311+G** basis set. The stability of the spin-restricted B3LYP solution was probed, and spin-unrestricted UB3LYP was employed if a triplet instability was detected. Harmonic vibrational frequencies confirmed that the structures corresponded to minima or first-order saddle points. The obtained zero-point vibrational energies were used for correcting the electronic energies of isomers. Intrinsic reaction coordinate calculations were performed to confirm that transition states indeed connected the expected reactive intermediates. Natural bond orbital (NBO)[27,28] analyses were performed for some species at the (U)B3LYP/6-311+G(d,p) level of theory by using the NBO 3.1[29] program.

Energies were refined by coupled-cluster theory involving single, double, and a perturbative estimate of triple excitations (CCSD(T)).[30,31] The coupled-cluster computations used Dunning's[32] correlation consistent triple-ζ basis set (cc-pVTZ) and were performed with the Molpro program.[33] Because the T_1 diagnostic values were larger than those recommended for a number of stationary points ($T_1 < 0.02$),[34] completely renormalized coupled cluster theory, CR-CCSD(T), was employed for some stationary points.[35–37] T_1 diagnostic values greater than a certain limit ($T_1 >$ 0.02) obtained in a coupled cluster calculation could signal an inadequacy of the single-reference-based coupled cluster method,[34] and showed the demand for a multiconfigurational treatment of the reference wavefunction. One way to describe the nondynamic electron correlation in diradicaloid species by using "black box" single-reference methods is the application of CR-CCSD(T), which has been shown to be able to describe diradicaloid and bond-breaking situations as reliably as CCSD(T) for closed-shell species.[35–37] The CR-CCSD(T) computations were performed with Dunning's[38] triple-ζ basis set with two sets of polarization functions on the hydrogen and heavy atoms with orbital exponents $\alpha_d(C) =$ 1.44, 0.36; $\alpha_d(O) = 2.56$, 0.64; $\alpha_d(B) = 1.00$, 0.25; $\alpha_d(N) = 1.96$, 0.49; and $\alpha_d(H) = 2.0$, 0.5, yielding the TZ2P[38] basis set. The renormal-

ized coupled cluster computations were performed with the GAMESS program.[39,40]

Because the relative energies of nitroso oxides **7**, computed at the CCSD(T) level, did not differ significantly from the renormalized coupled-cluster results, and because the appropriateness of the CCSD(T) method for the related HNOO molecule was demonstrated previously,[41] geometry optimizations were also performed at the CCSD(T) level of theory by using analytic gradients.[42] Dunning's DZP double-ζ basis set, with one set of polarization functions on the hydrogen and heavy atoms with orbital exponents $\alpha_d(C) = 0.654$, $\alpha_d(O) = 1.211$, $\alpha_d(B) = 0.386$, $\alpha_d(N) = 0.902$, and $\alpha_d(H) = 0.7$, was employed. Harmonic vibrational frequencies were obtained by finite differences of analytic gradients at the CCSD(T)/DZP level of theory. The CCSD(T) gradient computations were run with the CFOUR program.[43] The CCSD(T) harmonic vibrational frequencies for **7** were in better agreement with experiments than those at the B3LYP/6-311+G** level used previously,[12] whereas for **9** both methods gave very similar spectra.

The reaction of nitrene **6** with O_2 was investigated by using complete active space self-consistent field (CASSCF) theory. Relaxed potential-energy scan calculations were performed with the computational chemistry package ORCA[44] by using the valence double-ζ basis set def2-SV(P).[45] Because the CASSCF method considered nondynamic correlation only, the potential-energy curves obtained from the CASSCF relaxed scans were further refined with fully internally contracted *N*-electron valence state perturbation theory[46] (FIC-NEVPT2) in combination with the def2-SV(P) basis set, which also took into account dynamic correlation. The advantage of NEVPT2 is that it does not suffer from intruder states that could cause problems for other multireference perturbation theories, such as the more popular CASPT2 method.[47] Studies have shown that NEVPT2 performs similarly to CASPT2 or even better if intruder states caused problems for the latter method.[48,49]

Results and Discussion

Matrix-isolation experiments

Matrix-isolation infrared spectroscopic studies of boryl azide **5** were performed with different matrix hosts (Ar, N_2, and Ne, but only the Ar data are presented herein in detail; for very similar spectra obtained in N_2 and Ne, see Figures S2 and S3 in the Supporting Information) doped with 2–3% O_2. Irradiation of matrix-isolated precursor **5** with $\lambda = 254$ nm until it was completely bleached, as shown in Figure 1a, resulted in new IR bands. With the help of spectra computed at the CCSD(T)/DZP level of theory, it was confirmed that the species that formed after irradiation with $\lambda = 254$ nm were borylnitrene **6** and *anti*-nitritoborane **9a**.[12]

As reported previously,[12] nitrene **6** was consumed during annealing at 30 K for 30 min and new signals were observed, as shown in Figure 1b. One set of signals was the same as that which appeared after irradiation (Figure 1a) and was due to *anti*-nitritoborane **9a**. With the help of the computed spectrum (Figure 2b), the second set of new signals in Figure 1b was assigned to *anti*-nitroso-*O*-oxide **7a**, as done previously.[12] Furthermore, the matrix was irradiated at $\lambda = 254$ nm for 30 min and it was observed that **7a** was bleached, as observed in signals pointing downwards in Figure 1c. The set of signals pointing upwards (Figure 1c) is the same as that in both previous steps, and hence, was assigned to **9a**.

To further strengthen the assignments, heavy isotopic molecular oxygen, $^{18}O_2$, was used in one set of experiments with N_2 as a host material (Figure 3). The normal modes of calculated **7a** and **7a′** were compared and, as expected, normal modes with a significant contribution from the terminal NOO fragment of *anti*-nitroso-*O*-oxide showed significant shifts in their stretching frequencies. The experimental IR bands that were assigned to these normal modes (ν_{29}, ν_{25}, and ν_{23}, see Figure 4) in the case of experiments with $^{16}O_2$ were shifted if $^{18}O_2$ was employed and were assigned to **7a′**. The above observations further provide evidence in favor of the formation of *anti*-nitroso-*O*-oxide **7a** as one of the species upon annealing. All assignments of experimental IR spectra to their corresponding calculated spectra in Figures 2 and 3 are listed in Tables S3–S6 in the Supporting Information.

As reported earlier, the three isomers of **7** are very similar in energy.[12] However, in contrast to B3LYP, bisected isomer **7c** is the lowest energy isomer at the NEVPT2//CASSCF, CCSD(T)//B3LYP, and the CCSD(T) levels. Since the T_1 diagnostics of isomers **7** are higher (0.02 to 0.03) than those recommended (0.02),[34] the completely renormalized coupled-cluster method CR-CCSD(T) was employed as well. These results concurred with the CCSD(T) result that the relative energy of the isomers increased as **7c** < **7a** < **7b**. In addition, *syn*-isomer **7b** is a first-order saddle point at the CCSD(T)/DZP level of theory with a small imaginary vibrational frequency of 12*i* cm^{-1}. This explains why we do not detect formation of **7b** in our experiments. A comparison of the computed harmonic vibrational frequencies of **7a** and **7c** suggests that they differ to such an extent that the two isomers should be distinguishable (see Figure S5 in the Supporting Information). This leaves two important questions: 1) Why is the most stable isomer **7c** not detected? 2) How can the nitritoborane be formed thermally, that is, without photoexcitation? To further investigate the properties of **7a** and **7c**, additional computational investigations were performed as discussed in the next section.

Computational studies

To elucidate the mechanistic aspects for the formation of *anti*-nitritoborane **9a** after the reaction of triplet borylnitrene **6** and oxygen, a computational investigation was performed. This computational study is divided into two parts: 1) the formation of initial nitroso-*O*-oxide products upon annealing, as a result of the reaction between borylnitrene **6** and oxygen; and 2) the further reaction pathway that results in the formation of *anti*-nitritoborane **9a** as the final product.

The first reaction product formed from triplet CatBN **6** and triplet O_2, nitroso-*O*-oxide **7a**, has a singlet electronic ground state based on the (U)B3LYP and CCSD(T) computations. The triplet state is 26 and 40 kcal mol^{-1}, respectively, higher in energy. The singlet state of **7a** can be formed in a spin-allowed reaction from triplet nitrene **6** and triplet O_2 with all four open-shell electrons coupled to a singlet electronic state. It is clear that the electronic structure of the corresponding open-shell singlet state at a large distance is essentially impossible to describe with single-reference-based methods, such as

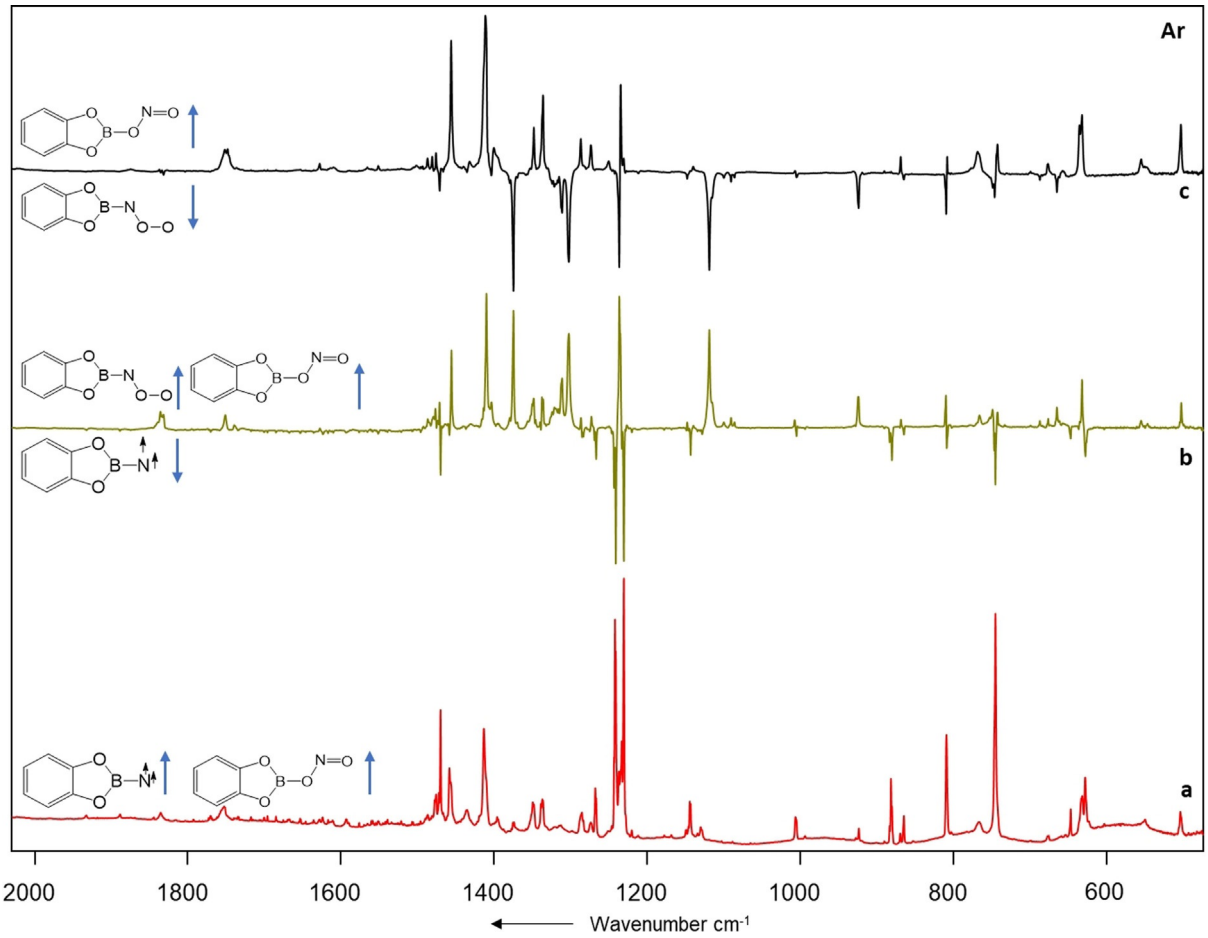

Figure 1. Infrared spectra obtained after irradiation of boryl azide **5** in O_2 (2–3%) doped argon matrix. a) After 60 min irradiation with $\lambda = 254$ nm at $T = 10$ K. b) Difference spectrum after annealing for 30 min at 30 K. c) Difference spectrum after irradiation with $\lambda = 254$ nm for 30 min.

Kohn–Sham DFT and Hartree–Fock reference-based coupled cluster methods. Hence, we employed the CASSCF method in conjunction with the def2-SV(P) basis set in CASSCF relaxed scan calculations with the N–O distance as the scan parameter, followed by single-point energy evaluations by using CASSCF-based second-order perturbation theory, NEVPT2. The choice of the proper active space for such a complex reaction with four open shells coupled to a singlet electronic state turned out to be challenging. Hence, we first selected the reaction of NH and O_2 as a model system that was previously studied by Talipov et al. using a full-valence active space and second-order perturbation theory (MCQDPT2//CASSCF).[11] Due to the small system size, we also performed the CASSCF and NEVPT2//CASSCF scan calculations with full-valence active space (18,13). The potential-energy curve (Figure 5a) shows that the barrier for the formation for imine peroxide, as a result of reaction of $NH + O_2$, is 7.1 kcal mol^{-1} at the CASSCF(18,13)/def-SV(P) level of theory. This was reduced to 0.4 kcal mol^{-1} by using NEVPT2/def-SV(P) single points. It has been reported that the formation of imine peroxide from NH and O_2 is barrierless under matrix-isolation conditions[10] and in the gas phase.[50] Hence, our refined barrier (0.4 kcal mol^{-1}) at the NEVPT2/def-SV(P) level is in agreement with regard to the reported experimental barriers for the formation of imine peroxide. It is also in agreement with closely related multiconfiguration perturbation theory (MCQDPT2; 1.4 kcal mol^{-1}) and multireference configuration interaction (MRCI; 0.8 kcal mol^{-1}) computations by using the full-valence active space reported by Talipov et al.[11]

A full-valence active space is computationally too demanding for treating the reaction of **6** + O_2, but close visual inspection of the relevant active-space orbitals of $NH + O_2$ allowed identification of relevant orbitals for the title reaction. Including the corresponding orbitals (see Figure S4 in the Supporting Information) in the active space of the **6** + O_2 system gave barriers for the formation of the *anti*- and bisected isomers of **7** of 7.1 and 13.4 kcal mol^{-1}, respectively, at the CASSCF(14,10)/def2-SV(P) level (Figure 5b,c). These barriers obtained from CASSCF calculations are too high to overcome under matrix-isolation conditions, but similar to the case of the $NH + O_2$ reaction, these barriers were reduced significantly after refinement with NEVPT2 (Figure 5a). The barriers of 0.4 kcal mol^{-1} for the formation of *anti*-isomer **7a** and 1.4 kcal mol^{-1} for bisected isomer **7c** (Figure 5b,c) are very small, similar to that of the $NH + O_2$ reaction at the same level of theory.

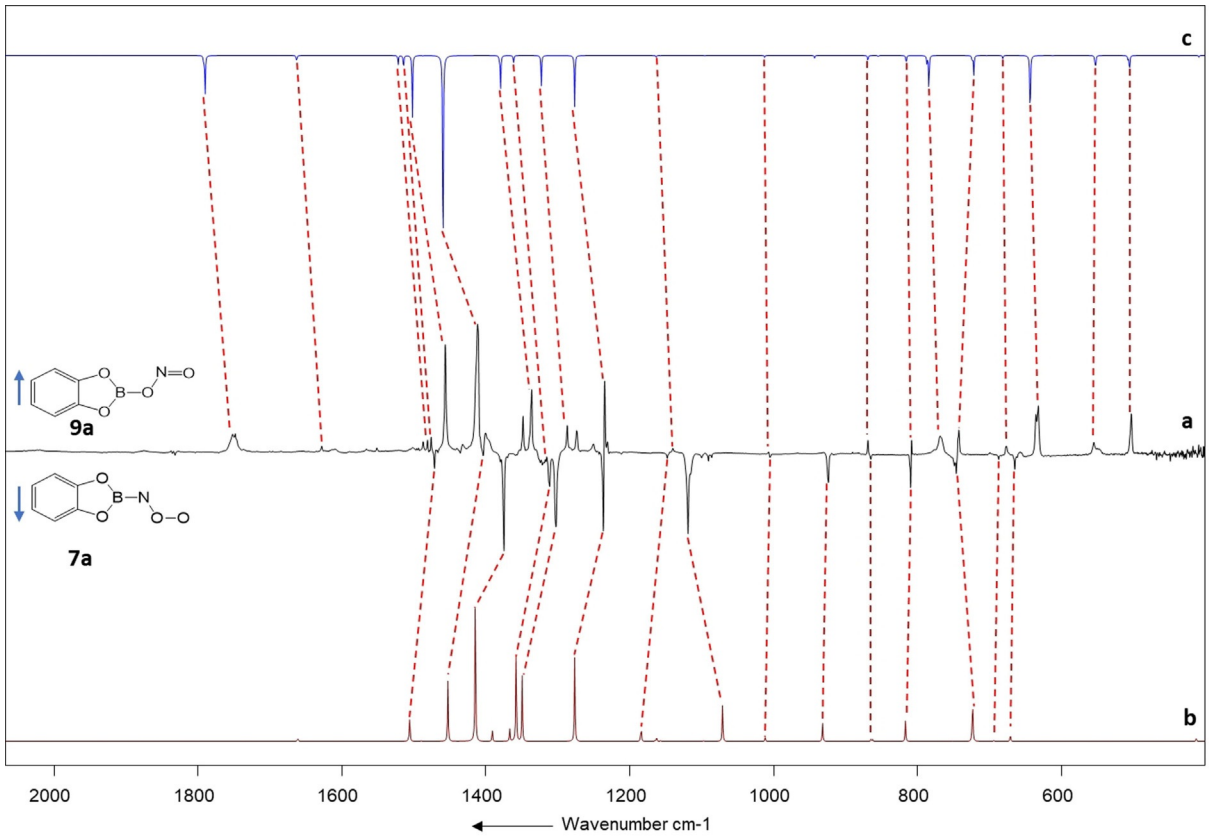

Figure 2. a) Difference IR spectrum after irradiation with $\lambda = 254$ nm for 30 min (following the annealing step). b) Calculated spectrum for ^{11}B and ^{10}B isotopologues (81:19) of *anti*-nitroso-*O*-oxide **7a** at the CCSD(T)/DZP level. c) Calculated spectrum for ^{11}B and ^{10}B isotopologues (81:19) of *anti*-nitritoborane **9a** at the CCSD(T)/DZP level.

The barriers for the formation of isomers **7a** and **7c** are low, but differ by roughly 1 kcal mol^{-1} at the present level of theory. It can be assumed that the barrier heights are further reduced by a more sophisticated treatment of electron correlation and expansion of the one-electron basis set, as shown by Talipov et al. for the NH + O_2 reaction, which does not rule out the absence of an activation barrier altogether.[11] Because both products **7a** and **9** are also formed in Ne matrix upon annealing to 10 K, the experiment suggests that the barriers are very small or may not even exist. That only isomer **7a** can be safely assigned in the experiments could be due to a kinetic preference for its formation, as suggested for the preferred formation of *trans*-HNOO in the case of the related HN + O_2 reaction.[10,11] However, we still need a channel for the formation of **9a** that has essentially no barrier. We therefore investigated the ground-state thermal reaction pathway from various geometrical isomers of nitroso-*O*-oxide (**7a**, **7b**, and **7c**) that finally resulted in *anti*-nitritoborane **9a** as the second part of our computational investigation. These calculations were performed at the CCSD(T)/cc-pVTZ//UB3LYP/6-311 + G** level, unless noted otherwise.

Despite their very similar energy contents (within 3 kcal mol^{-1}), the interconversions of **7a** to **7b** (a minimum at B3LYP, but a saddle point at CCSD(T)) or to **7c** have high energy demand (> 30 kcal mol^{-1}; Figure 6). Similarly, high barriers have been obtained computationally for the isomerization of *cis*- and *trans*-HNOO.[11] These interconversions are thus impossible thermally under cryogenic conditions.

The higher barriers associated with $\mathbf{TS_2}$ and $\mathbf{TS_3}$ are due to rotation about the N–O bonds that have pronounced double-bond character, according to their Wiberg bond indexes of 1.4–1.5 for all isomers **7a–c** (see Table S1 in the Supporting Information). On the other hand, transition-state $\mathbf{TS_4}$ corresponds to rotation about the B–N bond. NBO calculations showed that the Wiberg bond orders of the B–N bonds were in the range of 0.8–1.0 for isomers **7a–c** (see Table S1 in the Supporting Information). Hence, rotation about the B–N bond, as in $\mathbf{TS_4}$, is expected to be a low-energy process, whereas rotation about the N–O bond, as in $\mathbf{TS_2}$ and $\mathbf{TS_3}$, requires much more energy.

The bisected geometry **7c** provides the starting point for the low-barrier breaking of the B–N bond that results in a complex of **8** CatBO with NO (Figure 6). The barrier at the CCSD(T) level is only 0.8 kcal mol^{-1}. Because the T_1 diagnostic values (0.028 for **7c** and 0.029 for $\mathbf{TS_5}$) are larger than that of the generally accepted threshold of 0.02 suggested by Lee and Taylor,[34] we also performed CR-CCSD(T) computations that were significantly more robust for diradicaloids.[35–37] The classical barrier is < 0.1 kcal mol^{-1} at the CR-CCSD(T)/TZ2P//UB3LYP/6-311 + G** level, which confirms that thermal reaction of **7c** is clearly a low-energy process. The resulting complex **8** of the CatBO + NO radical pair is likely poorly described by CCSD(T)

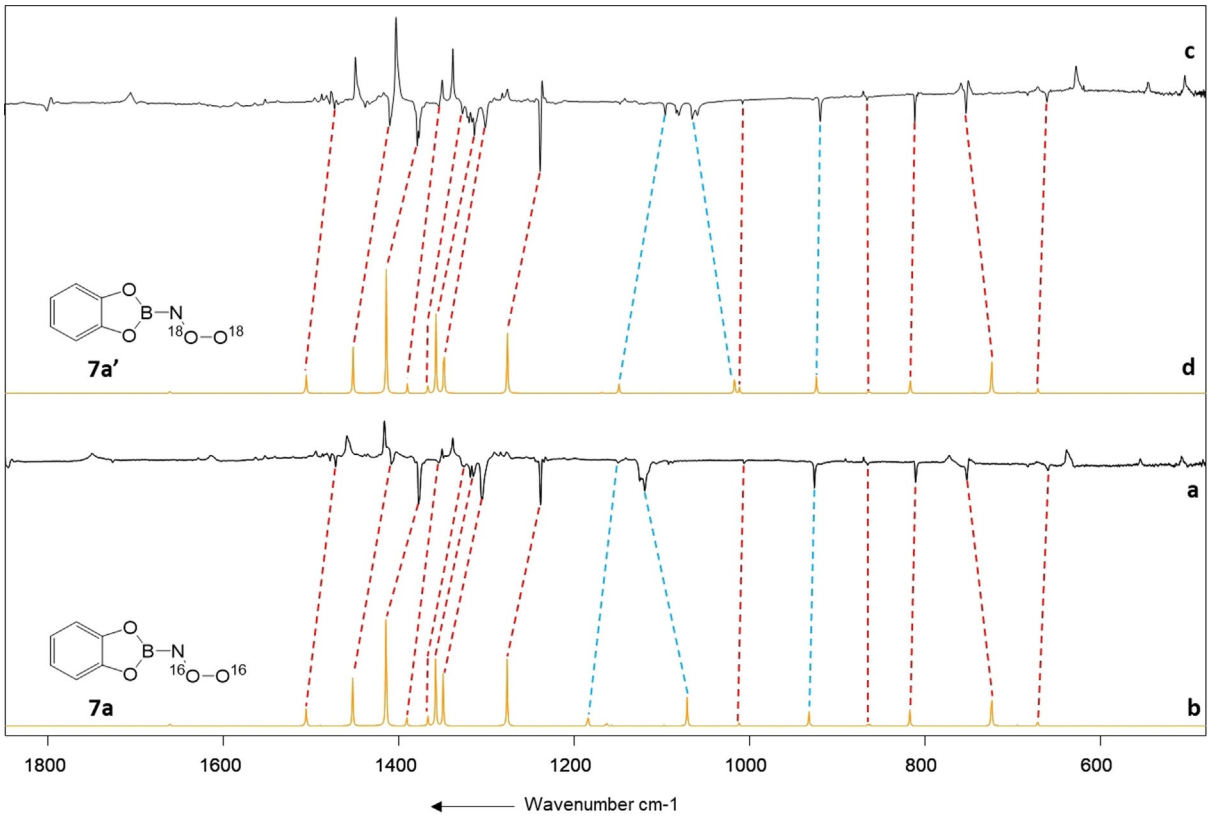

Figure 3. a) Difference spectrum after irradiation with $\lambda = 254$ nm for 40 min (following the annealing step). b) Calculated spectrum for ^{11}B and ^{10}B isotopologues (81:19) of *anti*-nitroso-*O*-oxide **7a** at the CCSD(T)/DZP level (with $^{16}O_2$). c) Difference spectrum after irradiation with $\lambda = 254$ nm for 30 min (following the annealing step). d) Calculated spectrum for ^{11}B and ^{10}B isotopologues (81:19) of *anti*-nitroso-*O*-oxide **7a**′ at CCSD(T)/DZP (with $^{18}O_2$).

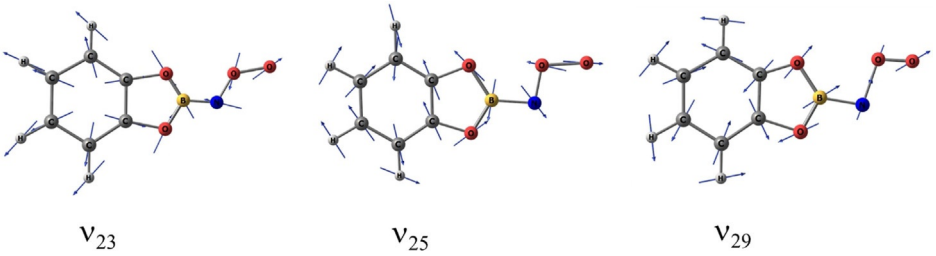

Figure 4. Normal modes with a significant contribution from the terminal NOO fragment of *anti*-nitroso-*O*-oxide **7a** (with $^{16}O_2$) calculated at the CCSD(T)/DZP level.

due to the large T_1 diagnostic of 0.032, and we consider the UB3LYP data more reliable. Complex **8** is stabilized by 59 kcal mol^{-1} relative to bisected isomer **7c**. Combination of the two radicals to give *syn*-nitritoborane **9b** is strongly exothermic and its barrier can likely be overcome by due to the energy gained by formation and the fixation in a matrix cage.[51] A very low barrier (0.2 kcal mol^{-1}) N–O bond rotation finally gives the more stable and experimentally observed *anti*-nitritoborane **9a**.

The formation of CatBO + NO from CatBN + OO can be regarded as a metathesis reaction that proceeds essentially without a barrier. Metal-free bond metathesis reactions involving boron are currently receiving attention.[52–58] For example, Kinjo et al. observed metal-free σ-bond metathesis in the reaction of alkoxyphosphine **10** and pinacolborane **11** that involved breaking of the P–O and B–H bonds, as shown in Scheme 2b.[52] This was explained by the high electrophilicity of boron on Bpin and hence, the formation of a strong B–O bond.[52] We observed similar reactivity for **6** + O_2 under matrix-isolation conditions, but in a stepwise manner. The high oxophilicity of the boron center plays an important role in attracting the terminal oxygen in **TS$_5$**, eventually leading to nitritoborane **9**, instead of the more often observed nitroborane.[7,8,59]

Conclusion

Detailed combined experimental and computational investigations reveal that borylnitrene shows high reactivity towards di-

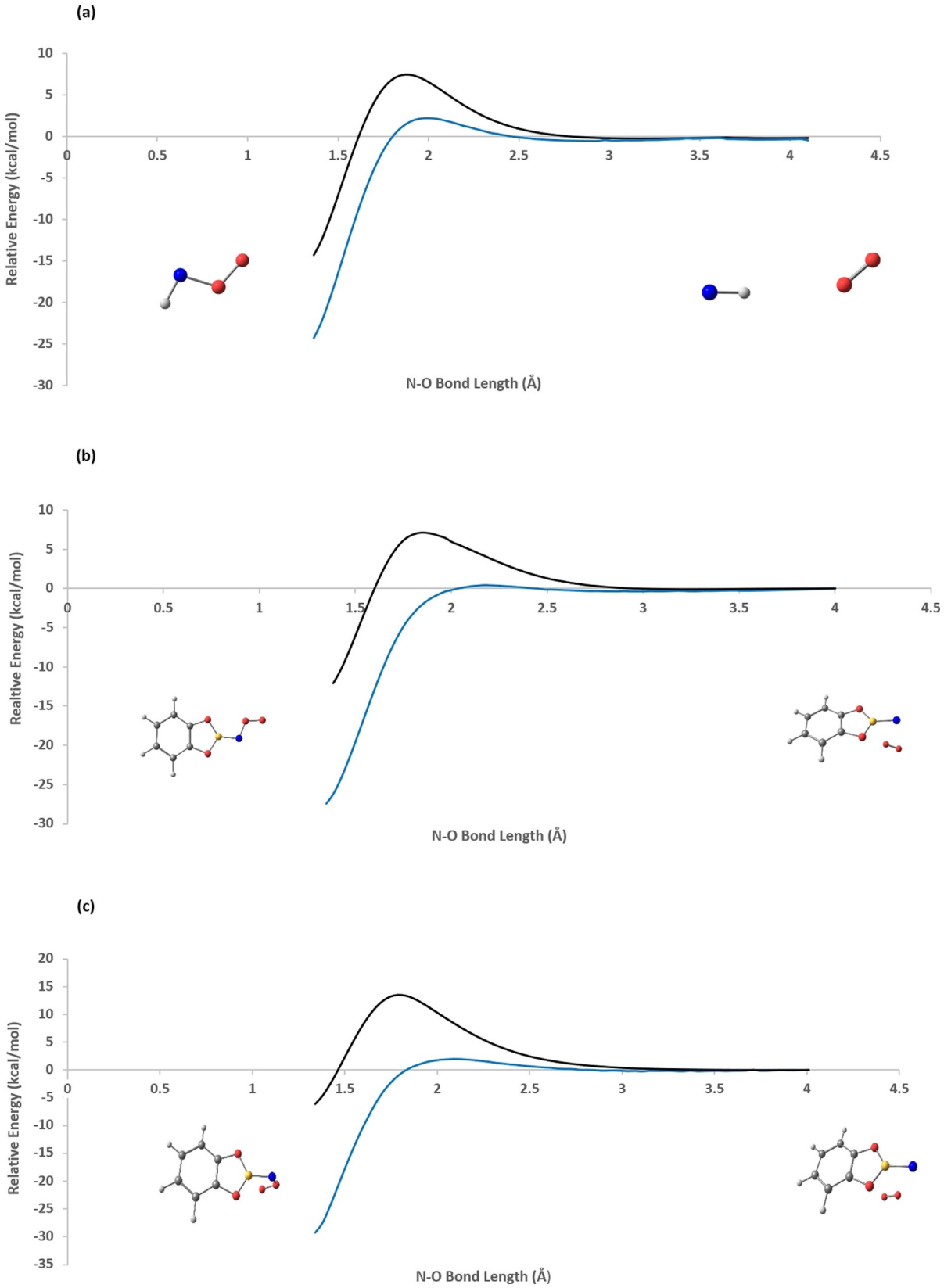

Figure 5. Potential-energy curves with the N–O bond as the scan parameter for reactions of nitrenes with O_2 computed at the CASSCF(n,m)/def2-SV(P) (black) and NEVPT2/def2-SV(P)// CASSCF(n,m)/def2-SV(P) (blue) levels. a) Formation of HNOO ($n=18$, $m=13$). b) Formation of *anti*-**7a** ($n=14$, $m=10$). c) Formation of bisected **7c** ($n=14$, $m=10$).

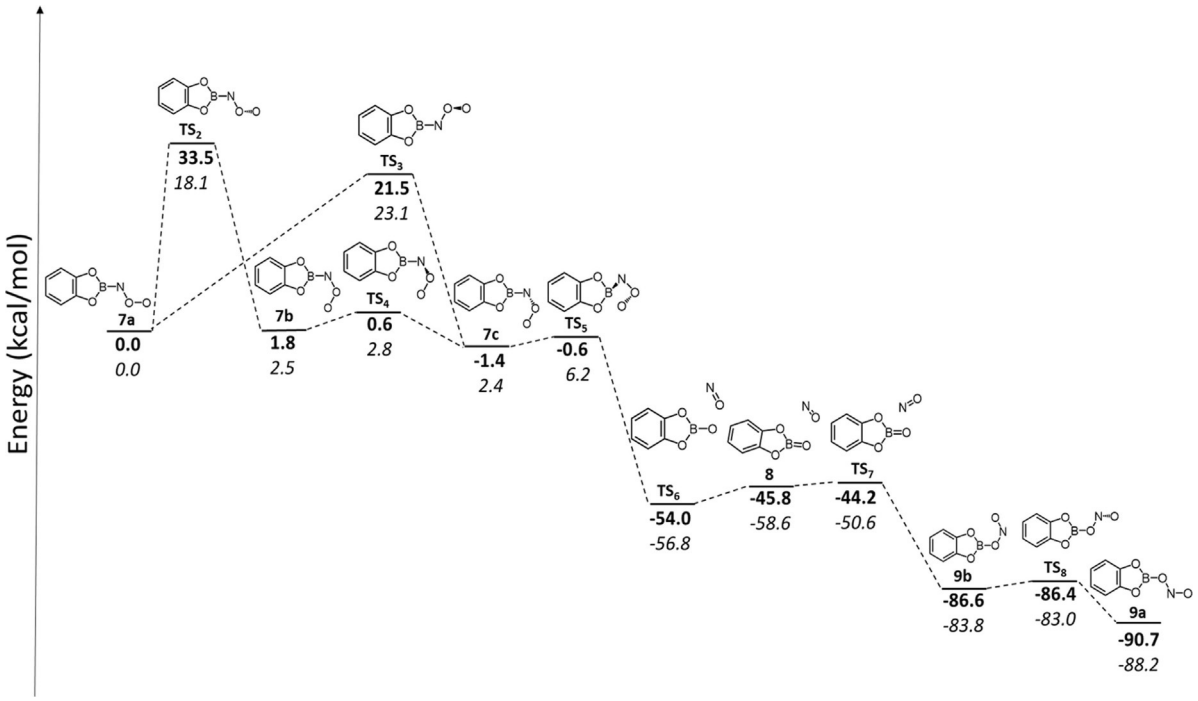

Figure 6. Potential-energy diagram showing the stationary points corresponding to various species involved and transition states for the formation of nitritoborane **9** after the reaction of triplet borylnitrene **6** and oxygen. All stationary points were calculated at the (U)B3LYP/6-311+G(d,p) (italics) and CCSD(T)/cc-pVTZ//(U)B3LYP/6-311+G(d,p) (bold) levels. Notably, the shape of the B3LYP potential-energy surface in the vicinity of **7b** is incorrect because it corresponds to a saddle point at CCSD(T)/DZP, which explains the unphysically low energy of $\mathbf{TS_4}$ at the CCSD(T)//B3LYP level.

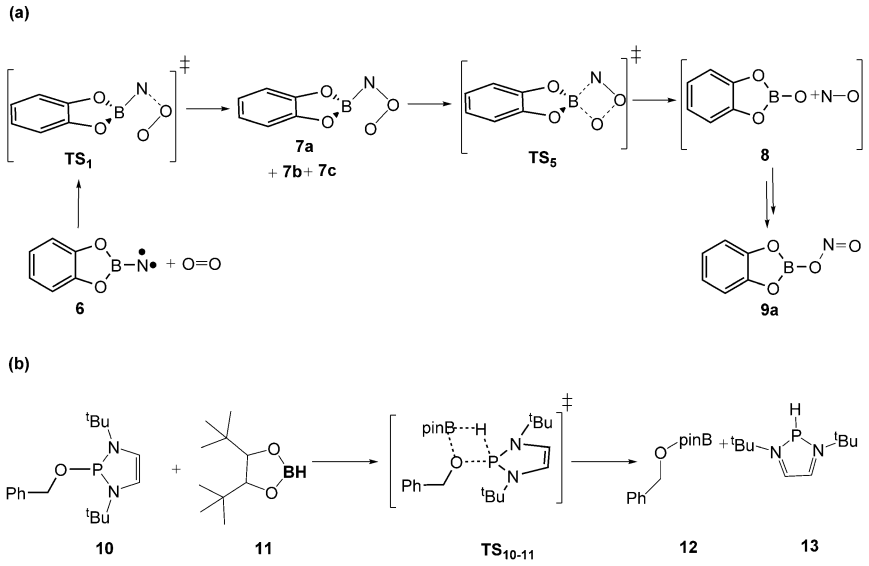

Scheme 2. a) Stepwise metathesis involving B–N and O–O bonds in current work driven by two transition states resulting in O_2 cleavage. b) The σ-bond metathesis between product **10** and pinacolborane **11**, resulting in breaking of the P–O bond, and hence, formation of **12** and **13**. Bpin = bis(pinacolato)diboron.

oxygen, even at very low temperatures, reminiscent of the behavior of the parent imidogen (NH), resulting in *anti*-nitroso-*O*-oxide **7a**. However, even the reaction of CatBN + O_2 → CatBO-NO (nitritoborane **9**) is feasible under very low temperature conditions. This unusual double insertion is stepwise and involves the metathesis reaction CatBN + OO → CatBO$^{\bullet}$ + $^{\bullet}$NO followed by radical combination in the matrix cage. Essential for this unprecedented reaction are the formation of bisected nitroso-*O*-oxide **7c** and the vanishingly low barrier for intramolecular attack of its terminal oxygen atom at the boron center. In contrast, *anti*-isomer **7a** behaves more conventionally. It is kinetically trapped under cryogenic conditions and is accessible to spectroscopy. It can form the more stable product **9** only after photoirradiation. We speculate that this induces iso-

merization and puts the system on the slippery slope towards the product.

The formation of **9** proceeds by the combination of CatBO and NO radicals in the stiff cryogenic matrix, which precludes separation of these species. It will be interesting to learn if this radical recombination would also be observable under more conventional solution-phase conditions, or if the heat of reaction of roughly -59 kcal mol^{-1} would result in radical pair separation by diffusion and allow observation of CatBO reactivity, for example, with solvent molecules.

Acknowledgements

This work was supported by the Deutsche Forschungsgemeinschaft and the Fonds der Chemischen Industrie. We are sincerely thankful to the state of Baden-Württemberg for bwHPC and to the German Research Foundation (DFG) through grant no. INST 40/467-1 FUGG for computation facilities. We would also like to thank Constanze Keck for her help in the synthesis of boryl azide **5**. Open access funding enabled and organized by Projekt DEAL.

Conflict of interest

The authors declare no conflict of interest.

Keywords: boron · density functional calculations · nitrenes · radicals · reaction mechanisms

[1] W. T. Borden, R. Hoffmann, T. Stuyver, B. Chen, *J. Am. Chem. Soc.* **2017**, *139*, 9010 – 9018.
[2] W. Sander, G. Bucher, S. Wierlacher, *Chem. Rev.* **1993**, *93*, 1583 – 1621.
[3] W. T. Borden, N. P. Gritsan, C. M. Hadad, W. L. Karney, C. R. Kemnitz, M. S. Platz, *Acc. Chem. Res.* **2000**, *33*, 765 – 771.
[4] M. S. Platz, *Acc. Chem. Res.* **1995**, *28*, 487 – 492.
[5] N. P. Gritsan, E. A. Pritchina, *Russ. Chem. Rev.* **1992**, *61*, 500 – 516.
[6] W. Sander, *J. Org. Chem.* **1989**, *54*, 333 – 339.
[7] E. A. Pritchina, N. P. Gritsan, T. Bally, *Phys. Chem. Chem. Phys.* **2006**, *8*, 719 – 727.
[8] J. Mieres-Pérez, E. Mendez-Vega, K. Velappan, W. Sander, *J. Org. Chem.* **2015**, *80*, 11926 – 11931.
[9] J. Liu, C. M. Hadad, M. S. Platz, *Org. Lett.* **2005**, *7*, 549 – 552.
[10] S. L. Laursen, J. E. Grace, R. L. DeKock, S. A. Spronk, *J. Am. Chem. Soc.* **1998**, *120*, 12583 – 12594.
[11] M. R. Talipov, S. L. Khursan, R. L. Safiullin, *J. Phys. Chem. A* **2009**, *113*, 6468 – 6476.
[12] H. F. Bettinger, H. Bornemann, *J. Am. Chem. Soc.* **2006**, *128*, 11128 – 11134.
[13] S. S. Ullah, P. K. Sharma, A. K. Guha, *Comput. Theor. Chem.* **2017**, *1115*, 307 – 312.
[14] H. F. Bettinger, M. Filthaus, H. Bornemann, I. M. Oppel, *Angew. Chem. Int. Ed.* **2008**, *47*, 4744 – 4747; *Angew. Chem.* **2008**, *120*, 4822 – 4825.
[15] H. F. Bettinger, M. Filthaus, P. Neuhaus, *Chem. Commun.* **2009**, 2186 – 2188.
[16] M. Filthaus, L. Schwertmann, P. Neuhaus, R. W. Seidel, I. M. Oppel, H. F. Bettinger, *Organometallics* **2012**, *31*, 3894 – 3903.
[17] M. Müller, C. Maichle-Mossmer, H. F. Bettinger, *Chem. Commun.* **2013**, *49*, 11773 – 11775.
[18] H. F. Bettinger, M. Filthaus, *Org. Biomol. Chem.* **2010**, *8*, 5477 – 5482.
[19] I. Fernández, F. P. Cossío, M. A. Sierra, *Chem. Rev.* **2009**, *109*, 6687 – 6711.
[20] M. T. Reetz, *Angew. Chem. Int. Ed. Engl.* **1972**, *11*, 129 – 130; *Angew. Chem.* **1972**, *84*, 161 – 162.
[21] M. T. Reetz, *Angew. Chem. Int. Ed. Engl.* **1972**, *11*, 130 – 131; *Angew. Chem.* **1972**, *84*, 163 – 163.
[22] W. Fraenk, T. Habereder, T. Klapoetke, H. Nöth, K. Polborn, *J. Chem. Soc. Dalton Trans.* **1999**, 4283 – 4286.
[23] I. R. Dunkin, *Matrix-isolation techniques: a practical approach*, Oxford University Press, New York, **2002**.
[24] A. D. Becke, *J. Chem. Phys.* **1993**, *98*, 5648 – 5652.
[25] C. Lee, W. Yang, R. G. Parr, *Phys. Rev. B* **1988**, *37*, 785 – 789.
[26] Gaussian 16, Revision C.01 M. J. Frisch, G. W. Trucks, H. B. Schlegel, G. E. Scuseria, M. A. Robb, J. R. Cheeseman, G. Scalmani, V. Barone, G. A. Petersson, H. Nakatsuji, X. Li, M. Caricato, A. V. Marenich, J. Bloino, B. G. Janesko, R. Gomperts, B. Mennucci, H. P. Hratchian, J. V. Ortiz, A. F. Izmaylov, J. L. Sonnenberg, Williams, F. Ding, F. Lipparini, F. Egidi, J. Goings, B. Peng, A. Petrone, T. Henderson, D. Ranasinghe, V. G. Zakrzewski, J. Gao, N. Rega, G. Zheng, W. Liang, M. Hada, M. Ehara, K. Toyota, R. Fukuda, J. Hasegawa, M. Ishida, T. Nakajima, Y. Honda, O. Kitao, H. Nakai, T. Vreven, K. Throssell, J. A. Montgomery, Jr., J. E. Peralta, F. Ogliaro, M. J. Bearpark, J. J. Heyd, E. N. Brothers, K. N. Kudin, V. N. Staroverov, T. A. Keith, R. Kobayashi, J. Normand, K. Raghavachari, A. P. Rendell, J. C. Burant, S. S. Iyengar, J. Tomasi, M. Cossi, J. M. Millam, M. Klene, C. Adamo, R. Cammi, J. W. Ochterski, R. L. Martin, K. Morokuma, O. Farkas, J. B. Foresman, D. J. Fox, Wallingford, CT, **2016**.
[27] J. P. Foster, F. Weinhold, *J. Am. Chem. Soc.* **1980**, *102*, 7211 – 7218.
[28] J. E. Carpenter, F. Weinhold, *THEOCHEM* **1988**, *169*, 41 – 62.
[29] NBO Version 3.1., E. D. Glendening, A. E. Reed, J. E. Carpenter, F. Weinhold, **2003**, Gaussian Inc., Pittsburgh.
[30] K. Raghavachari, G. W. Trucks, J. A. Pople, M. Head-Gordon, *Chem. Phys. Lett.* **1989**, *157*, 479 – 483.
[31] R. J. Bartlett, J. D. Watts, S. A. Kucharski, J. Noga, *Chem. Phys. Lett.* **1990**, *165*, 513 – 522.
[32] T. H. Dunning, Jr., *J. Chem. Phys.* **1989**, *90*, 1007 – 1023.
[33] H.-J. Werner, P. J. Knowles, G. Knizia, F. R. Manby, M. Schütz, *WIREs Comput. Mol. Sci.* **2012**, *2*, 242 – 253.
[34] T. J. Lee, P. R. Taylor, *Int. J. Quantum Chem.* **1989**, *36*, 199 – 207.
[35] P. Piecuch, S. A. Kucharski, K. Kowalski, M. Musiał, *Comput. Phys. Commun.* **2002**, *149*, 71 – 96.
[36] K. Kowalski, P. Piecuch, *J. Chem. Phys.* **2000**, *113*, 18 – 35.
[37] K. Kowalski, P. Piecuch, *J. Chem. Phys.* **2000**, *113*, 5644 – 5652.
[38] T. H. Dunning, *J. Chem. Phys.* **1971**, *55*, 716 – 723.
[39] M. W. Schmidt, K. K. Baldridge, J. A. Boatz, S. T. Elbert, M. S. Gordon, J. H. Jensen, S. Koseki, N. Matsunaga, K. A. Nguyen, S. Su, T. L. Windus, M. Dupuis, J. A. Montgomery, Jr., *J. Comput. Chem.* **1993**, *14*, 1347 – 1363.
[40] M. S. Gordon, M. W. Schmidt in *Theory and Applications of Computational Chemistry* (Eds.: C. E. Dykstra, G. Frenking, K. S. Kim, G. E. Scuseria), Elsevier, Amsterdam, **2005**, pp. 1167 – 1189.
[41] R. L. DeKock, M. J. McGuire, P. Piecuch, W. D. Allen, H. F. Schaefer, K. Kowalski, S. A. Kucharski, M. Musiał, A. R. Bonner, S. A. Spronk, D. B. Lawson, S. L. Laursen, *J. Phys. Chem. A* **2004**, *108*, 2893 – 2903.
[42] G. E. Scuseria, *J. Chem. Phys.* **1991**, *94*, 442 – 447.
[43] J. F. Stanton, J. Gauss, L. Cheng, M. E. Harding, D. A. Matthews, P. G. Szalay, CFOUR, Coupled-Cluster techniques for Computational Chemistry, Version 2.00beta, for the updates, see http://www.cfour.de.
[44] F. Neese, *WIREs Comput. Mol. Sci.* **2012**, *2*, 73 – 78.
[45] F. Weigend, R. Ahlrichs, *Phys. Chem. Chem. Phys.* **2005**, *7*, 3297 – 3305.
[46] C. Angeli, R. Cimiraglia, J.-P. Malrieu, *J. Chem. Phys.* **2002**, *117*, 9138 – 9153.
[47] C. Angeli, R. Cimiraglia, S. Evangelisti, T. Leininger, J.-P. Malrieu, *J. Chem. Phys.* **2001**, *114*, 10252 – 10264.
[48] C. Camacho, R. Cimiraglia, H. A. Witek, *Phys. Chem. Chem. Phys.* **2010**, *12*, 5058 – 5060.
[49] R. W. A. Havenith, P. R. Taylor, C. Angeli, R. Cimiraglia, K. Ruud, *J. Chem. Phys.* **2004**, *120*, 4619 – 4625.
[50] T. Fueno, K. Yokoyama, S.-Y. Takane, *Theor. Chim. Acta* **1992**, *82*, 299 – 308.
[51] Z. Wu, C. Chen, J. Liu, Y. Lu, J. Xu, X. Liu, G. Cui, T. Trabelsi, J. S. Francisco, A. Mardyukov, A. K. Eckhardt, P. R. Schreiner, X. Zeng, *J. Am. Chem. Soc.* **2019**, *141*, 3361-3365.
[52] C. C. Chong, H. Hirao, R. Kinjo, *Angew. Chem. Int. Ed.* **2015**, *54*, 190 – 194; *Angew. Chem.* **2015**, *127*, 192 – 196.
[53] Y. Wang, W. Chen, Z. Lu, Z. H. Li, H. Wang, *Angew. Chem. Int. Ed.* **2013**, *52*, 7496 – 7499; *Angew. Chem.* **2013**, *125*, 7644 – 7647.

[54] H. Braunschweig, A. Damme, C. Hoerl, T. Kupfer, J. Wahler, *Organometallics* **2013**, *32*, 6800-6803.
[55] C.-Y. Lee, S.-J. Ahn, C.-H. Cheon, *J. Org. Chem.* **2013**, *78*, 12154-12160.
[56] Q. Yin, S. Kemper, H. F. T. Klare, M. Oestreich, *Chem. - Eur. J.* **2016**, *22*, 13840-13844.
[57] Y. K. Loh, K. Porteous, M. A. Fuentes, D. C. H. Do, J. Hicks, S. Aldridge, *J. Am. Chem. Soc.* **2019**, *141*, 8073 – 8077.
[58] S. A. Iqbal, J. Pahl, K. Yuan, M. J. Ingleson, *Chem. Soc. Rev.* **2020**, *49*, 4564-4591.
[59] N. Sawwan, A. Greer, *Chem. Rev.* **2007**, *107*, 3247 – 3285.

Manuscript received: May 18, 2020
Revised manuscript received: June 11, 2020
Version of record online: September 9, 2020